

## 2.6. Application of the ion bombardment technique to study the behavior of rare gases in $\text{UO}_2$ ; comparison with reactor irradiation and the influence of irradiation on fission gas bubbles.\*

H. MATZKE, *European Institute for Transuranium Elements, Karlsruhe, W. Germany*

### *Abstract*

The ion bombardment technique is applied to study the behavior of the fission gases Xe and Kr in  $\text{UO}_2$ , a question of considerable importance in technology due to the contribution of the gases to the swelling of the fuel. The system of Stages in gas release is used to discuss the experimental results. In the order of increasing temperatures, Stages IA, IIA, IIB and III are observed, whereas Stage IB is missing. Stage IA release occurs at low temperatures, starting at about  $600^\circ\text{C}$ , and is probably due to gas located very near to the surface: it can explain the so called "burst" — effect observed in many studies, i. e. a fast initial release in isothermal experiments. Stage IB release is absent since no gross structural damage is formed in  $\text{UO}_2$  during bombardment, the ratio of the crystallization temperature,  $T_c$ , and the melting point,  $T_m$ , being low ( $<0.30$ ).

Normal volume diffusion of single gas atoms (Stage IIA) proceeds with an activation enthalpy,  $\Delta H$ , of  $3.9 \pm 0.2$  eV. Doping and channeling experiments together with results obtained following bombardment at different temperatures up to  $1000^\circ\text{C}$  suggest that the rare gas atoms migrate in small equilibrium vacancy clusters, e. g. in Schottky trios. At higher gas and damage concentrations, the gas mobility is retarded due to gas—gas or gas—damage interactions (Stage IIB), the most effective trapping centers probably being bigger vacancy clusters and loops.

At high gas concentrations and high temperatures, gas atoms interact with other gas atoms to form bubbles. The nucleation and mobility of these bubbles is discussed as well as their stability under irradiation. Recently, it was demonstrated that gas atoms can be redissolved by fission events. The implications on swelling, i. e. on the dimensional stability of the fuel, are discussed. The present knowledge of the mobility of fission gases in  $\text{UO}_2$  is shown to be adequate to qualitatively explain and predict the behavior of the fuel element in the reactor though important aspects have still to be investigated in more detail.

## 2.7. Ion irradiation induced damage in pure gold thin films

A. R. BAYLY and G. CARTER, *Dept. of Elec. Eng., University of Salford, Lancs. U. K.*

### 1. Introduction

The irradiation of solids with electrons and light particles such as protons, neutrons and deuterons, has been successfully employed for about twenty years, to study the generation and behaviour of effects in solids since, when such particles, accelerated to high energy collide with the atoms of a solid lattice, sufficient energy can be transferred to cause displacement of these atoms and thus the production of defects. Specification of the incident particle energy can give direct information about the energies required for atomic displacement and post irradiation thermal annealing studies can reveal the nature of the defects produced. The nature of these observations range from direct microscopic scale

\* To be published in the Book of Lectures of the Summer School on Physics of Ionized Gases, Herceg Novi, 1970.

investigations using electron and field ion microscopic techniques to measurements of macroscopic property changes which depend upon the defect state of the solid, such as electrical resistivity, internal friction, etc.<sup>1)</sup>

In such studies and particularly for electrons, relatively high particle energies are required (e.g. in the order of 1 MeV), since the energy transfer efficiency to lattice atoms is low but this also has an advantage in that the range of these high energy projectiles in a solid is large, so that relatively thick samples can be used and the defects are formed homogeneously throughout the solid.

More recently, studies of defect formation by heavier energetic particles, have become fashionable as a result of the more readily available technology for heavy ion generation and manipulation and a widespread interest in the interaction of heavy ions with solids because of its potential technological importance in such areas as the implantation of semiconductors. Since energy transfer from a heavy ion to a lattice atom is generally rather efficient, quite low ion energies may be employed (in the order of keV's) but there is the disadvantage that such low energy heavy ions possess commensurately low ranges in solids (tens to hundreds of Angstroms). Consequently, in order to obtain meaningful data from heavy ion injection studies, it is necessary to use thin targets, so that any property change induced by defect formation is not shunted by the undamaged bulk of the target beyond the ion range, or that after irradiation, the damaged layer can be directly observed after removal of the undamaged bulk. This latter technique is used for the electron microscopic observations of defect formation induced by heavy ion irradiation whilst, for experiments in which a property change is studied as a consequence of defect formation, it has been necessary to use initially thin targets such as evaporated films.

Several investigators<sup>2,3,4)</sup> have reported experiments with metallic films in this category of work, where the property change observed was the electrical resistivity. In these studies, it was found that resistivity generally increases as a function of ion dose, due to defect formation and sputter thinning of the films.

The investigation of Teodosić<sup>2)</sup> and Navinšek and Carter<sup>3)</sup> showed, however, that there was frequently an initial decrease of resistance with ion dose and the latter authors ascribed this effect to ion beam removal of surface adsorbed gases from the films. The present study was, therefore, undertaken, in which every precaution was taken to ensure film cleanliness and purity before, during and after ion bombardment, in order that any spurious effects due to surface contamination should be minimised — and this communication reports the results of this study using low energy inert gas ions incident on gold films.

## 2. Experimental Apparatus and Techniques

### a) Vacuum system

In order that the gold films should be as free from surface contaminants as possible it is necessary that these should be produced and maintained during ion bombardment and subsequently under ultra high vacuum conditions. Consequently, the experiments were conducted in a bakeable stainless steel target chamber, shown in Fig. 1, which was pumped via a liquid nitrogen cold trap by an oil diffusion pump. Using conventional pumping and baking schedules, the pressure in the target chamber could be reduced to the low  $10^{-9}$  torr regime, which was monitored both with a Bayard-Alpert type total pressure gauge and a 2 cm

radius bakeable mass spectrometer which were mounted on side flanges of the target chamber. The films were produced by evaporation from a specially designed boat which ensured uniformity of deposit and incorporated an electron gun for vapour stream ionisation, onto glass substrates. The evaporator assembly was

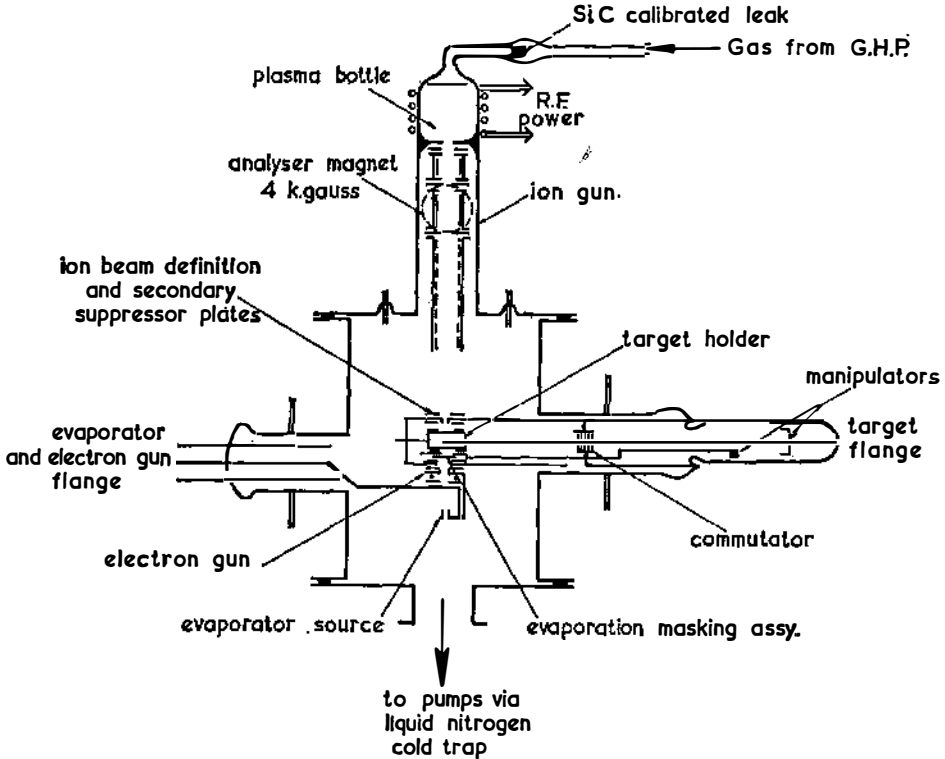


Fig. 1 The U. H. V. system.

mounted and supplied with electrical power via glass-metal feedthroughs in a further flange at the side of the vacuum chamber. Eight glass substrates were mounted on a rotatable assembly, so that eight films could be produced consecutively by rotation of the appropriate substrate into the vapour stream and subsequently consecutively bombarded by further rotation into the ion beam. Resistivity monitoring apparatus was connected to each film from outside the vacuum system via a multi-feedthrough flange which fed silver sheet brushes within the vacuum system. These brushes, in turn, contacted a set of commutators, again with silver sheet contacts, which were individually connected to each film. Thus, upon rotation of the glass substrate assembly, which was accomplished by an external magnetic coupling facility, each film was consecutively connected to the resistance monitoring equipment. Suitable masking arrangements were fitted to the rotary target holder, to allow for precise definition of the area of the films during deposition and the area of the films exposed to ion bombardment. Two potential leads and two current leads were connected to each film, so that resistivity could be monitored under constant low current condi-

tions to minimise heating of the films and consequent thermal resistance changes. The temperature of the films was not, in fact, measured directly but was assessed by using a further thick film of gold (several thousand angstroms thick) on a separate glass substrate mountable in an identical position to any of the test films. The resistance of this film, which received no irradiations, was then monitored and from the known temperature coefficient of resistance of gold, it was possible to estimate the temperature of the film under the required conditions.

Ion irradiations were accomplished by extracting and focusing ions, in the energy range 300 eV—3 keV, from an R. F. ion source mounted at the top of the vacuum chamber. A small Wien filter allowed mass analysis of the beam before entrance into the target chamber, whilst in addition, only spectroscopically pure inert gas ions were used for irradiations to minimise film contamination effects, thus, although the inert gas particle pressure in the target area rose to the order of  $10^{-5}$  torr during ion irradiation, the active gas partial pressure remained below  $10^{-9}$  torr. The ion beam energy was defined by the target potential relative to the ion source extraction potential but as with most R. F. type plasma sources, there was a potential distribution within the plasma giving rise to an ion energy spread of the order of 100 eV at all ion energies. The geometry of the ion beam striking the film target was defined by using a somewhat defocused ion beam and passing this through a slit before the target, whilst a further plate containing an aperture of larger dimensions than this beam defining slit was mounted immediately adjacent to the target film to suppress or collect secondary particles from the target.

#### b) Sample preparation

Before film evaporation, the glass substrates were carefully cleaned by hot detergent and deionized water treatments and final drying with lint free tissue and under an infra red lamp. These substrates had dimensions of  $10 \text{ mm} \times 2.3 \text{ mm} \times 1.0 \text{ mm}$  and after cleaning gold contacts were evaporated at a pressure of  $\sim 10^{-5}$  torr, at each end of the longest dimension. The dimensions of each contact were then  $2.5 \text{ mm} \times 2.3 \text{ mm}$  and each was several thousand angstroms thick. These substrates were then mounted in the vacuum system and spring loaded silver contacts connected to the gold contact pads. After system pumping and baking, with the gold vapour source heated to just below its normal evaporation temperature, to achieve optimum degassing, the system pressure finally fell to the low  $10^{-9}$  torr range, with the major residual gas components being CO and H<sub>2</sub>O. Gold evaporations were then commenced with the target assembly at about 200°C and with the vapour beam ionizer activated. With this arrangement, it was possible to monitor and control the constancy of evaporation rate (but, of course, not necessarily the deposition rate) and during the period the system pressure rose instantaneously to the  $10^{-7}$ — $10^{-6}$  torr range (mostly H<sub>2</sub>O and CO) but declined rapidly. The thickness of the evaporated films was generally of the order of 500 Å (as measured by a Talystep, a sensitive mechanical thickness monitor) and these covered the area between the gold contacts and partly overlaid the contacts. After evaporation, the films were annealed and aged at 350°C by electron beam heating from the vapour stream ionizer source, after which treatment the film resistance remained stable to 0.01% for the short periods of the experimental time. (This instability itself probably resulting from diurnal temperature fluctuations.)

The structures of the films were studied by a Talystep thickness monitor and low energy proton back-scattering in a proton scattering microscope from which it was deduced that the films were certainly continuous and of a polycrystalline habit, probably consisting of an array of randomly oriented crystallites of the order of 3000 Å diameter but with a preferred orientation of the [111] plane parallel to the substrate surface.

### c) Ion bombardment schedules

As noted earlier, the ion beam striking the target was defined by a slit which caused the beam to impinge on the central region of the film over the complete 2–3 mm width of the film, whilst the narrower dimension of the bombarded area was approximately 0.2 mm. Basically, three types of experiment were conducted: (1) Measurement of the secondary negative and positive particle emission from the film, as a result of  $A^+$  or  $Xe^+$  ion bombardment in the energy range 0.3 → 3.0 keV by monitoring both the target and collector plate currents for variable voltage differences between these. Such experiments were conducted separately and during the major investigations of (2) the change in film resistance as a function of ion dose for bombardments by  $A^+$  or  $Xe^+$  ions in the energy range 0.3 → 3.0 keV and (3) the changes in film resistance due to successive bombardments with different energy ions of the same type. In this type of study, the change in resistance was monitored as a function of ion dose at a given ion energy, then the ion energy was reduced and further resistance changes observed.

The resistance of the film was monitored by passing a constant low direct current ( $\sim 10\text{mA}$ ) through the film and determining the voltage drop across the film. In fact, a backing off circuit was employed, so that after initial resistance determination before bombardment, the initial voltage drop was backed off across the film and any subsequent changes in the measured voltage across the film were thus due to resistance changes. These changes were measured with a microvoltmeter and displayed, as a function of time on a pen recorder. This monitoring circuit was connected to ground via a  $10^5\Omega$  resistor, so that the incident ion current to the target or particle current to the collector registered a measurable voltage drop across this resistor, which was simultaneously displayed upon the pen recorder, together with the resistance changes. Extensive screening and decoupling procedures were necessary to obtain accurate ion beam currents and resistance changes during operation of the R.F. source but it was found that errors originating from this source could be reduced to the order of 0.01%.

## Results and Discussion

### a) Secondary particle emission processes

It is initially instructive to discuss the secondary particle emission results, since these also indicate the freedom of the subsequent data on resistance changes from gaseous contamination effects, a principal aim of our studies. In order to measure the negative (electron) emission coefficient  $\gamma_-$  from the target and the positive emission coefficient  $\gamma_+$ , observations of the currents striking both the target and the collector were made for voltage values of the

latter both positive and negative, with respect to the target. It was found that, with an applied potential difference  $\gtrsim \pm 20$  V, the target current remained constant indicating that at and above these voltages the collector received either all emitted electrons or positively charged particles. From the ratio of the collector currents at saturation to the sum of the collector and target currents  $\gamma_-$  and  $\gamma_+$  were evaluated with the following results.  $\gamma_-$  increases for a gold film from approximately 0.05 at 300 eV as a linear function of energy to 0.22 at 3.0 keV for  $A^+$  ions and from approximately 0.01 at 300 eV to 0.06 at 3 keV, again linearly, for  $Xe^+$ . This ion energy and mass dependence is as expected for kinetic emission of electrons, the more important process in this energy regime.  $\gamma_+$  also increases linearly with energy for  $A^+$  ions from 0.05 at 300 eV to 0.1 at 3.0 keV. Equally important was the observation that for an atmospherically contaminated film, the values of  $\gamma_-$  and  $\gamma_+$  were higher by factors of between 3 and 10, depending upon ion energy than those for clean, carefully prepared films. The importance of this observation lies in the fact that when clean films were bombarded and  $\gamma_-$  and  $\gamma_+$  observed over long periods of time, they were only found to diminish slightly indicating the cleanliness of the film. Indeed, the initial reduction in both  $\gamma_-$  and  $\gamma_+$  was rapid followed by a slower fall and finally a constant value of  $\gamma_-$  and  $\gamma_+$ . If films were then allowed to reside for several hours before rebombardment no initial rapid reduction occurred, further confirming the lack of surface contamination. Indeed, this leads one to believe that both  $\gamma_-$  and  $\gamma_+$  are reduced by continued ion bombardment, probably as a result of randomisation of the crystal lattice by defect formation, since it is well known<sup>9</sup> that emission from a good crystal is lower when ions are injected in channel directions than when ions are injected randomly. These observations are also important to the subsequent discussion where it will be shown that changes in ion energy result in resistance increases, which cannot be expected due to contamination effects. Finally, measurements of  $\gamma_-$  and  $\gamma_+$  allowed accurate specification of the true target beam currents which were found to be constant to within a few percent and these values are therefore used in the following discussion.

#### b) Sputtering

When measurements were made of changes of resistance with increasing ion dose for any ion of fixed energy, the following qualitative behaviour was observed. Initially, the resistance increases rather rapidly, then the rate declines, reaches a quasiequilibrium value and then commences to rise rapidly again. This behaviour contrasts sharply with that observed by earlier workers using undoubtedly contaminated films where the initial effect was a resistance decrease before the first increase phase. Only in experiments where either the target was deliberately contaminated or the ion beam was deliberately contaminated were similar effects observed in the present work, thus substantiating Navinšek and Carter's<sup>3</sup> proposal that ion beam decontamination of the surface is responsible for the initial resistance decrease and further indicating the film purity in the present study. The initial resistance increase and quasisaturation phase will be considered shortly, at this stage, we shall further consider the final resistance increase. This region is undoubtedly, as suggested by Navinšek and Carter, a result of sputtering of the film, since topographs of the surface taken with a Talystep during this phase, indicate the erosion of the surface uniformly where

the ion beam strikes, until eventually, all the film is removed, which is also indicated by an increase in film resistance towards infinity.

Of course sputtering will occur throughout bombardment and in order to properly interpret the initial resistance phases, the contribution of sputtering to this region must be assessed. Consequently, from the final resistance rise phase, sputtering coefficients were deduced and these used to evaluate the effects of sputtering in the earlier resistance change phases.

Since the ion beam is of rectangular cross-section it removes (as substantiated by the Talystep topographic profile) a rectangular section from the gold film. Consequently, if the initial film thickness is  $d$  and the beam removes a depth  $x$  of film in time  $t$ , conduction between the gold pad contacts only takes place in the uneroded section of the film of thickness  $d-x$ .

If the resistivity of the film is  $\rho$ , the resistance of a section thickness  $x$  is

$$R = \rho(d-x)^{-1} \Omega/\text{square}. \quad (1)$$

Further if the sputtering coefficient is  $S$  gold atoms removed per incident ion from a target of density  $N$  atoms/cm<sup>3</sup> by a beam of  $\Phi$  ions/cm<sup>2</sup>, then in a time  $t$ , the depth of gold removed is given by

$$x = \vartheta S \cdot N^{-1} \cdot t = \Phi S N^{-1}, \quad (2)$$

where  $\vartheta t = \Phi$  the integrated ion dose.

Combining (1) and (2) and differentiating,

$$\frac{dR}{d\Phi} = \rho S N^{-1} (d - \Phi S N^{-1})^{-2}. \quad (3)$$

Integrating this expression then shows that the fractional change in resistivity from the initial value  $\frac{\delta R}{R}$ , for an ion dose  $\Phi$ , is given by

$$\frac{\delta R}{R} = \frac{\Phi S}{Nd}. \quad (4)$$

Thus a plot of  $\frac{\delta R}{R}$  as a function of ion dose should be linear, the slope giving the value of  $S$ . There is some imprecision in this derivation, since it ignores the fact that at small film thicknesses, electron scattering at the film surfaces assumes importance in comparison with the bulk scattering determining resistivity.

An estimate of this error can be included using an approximation for this skin effect by Chopra and Randlett<sup>6)</sup> and for the present films this error is estimated to be below 25% if equation (4) is used.

Experimental measurements of  $\frac{\delta R}{R}$  as a function of ion dose, in the high dose region ( $10^{15} \rightarrow 3 \times 10^{16}$  ions/cm<sup>2</sup>) are shown in Fig. 2 for A<sup>+</sup> and Xe<sup>+</sup> ions at several different energies and the linear dependence of equation (4) is clearly obeyed. From such curves,  $S$  has been derived for A<sup>+</sup> and Xe<sup>+</sup> ions, using measurements of initial film thickness from Talystep measurements and the initial film resistance and these are compared in Fig. 3 with other published

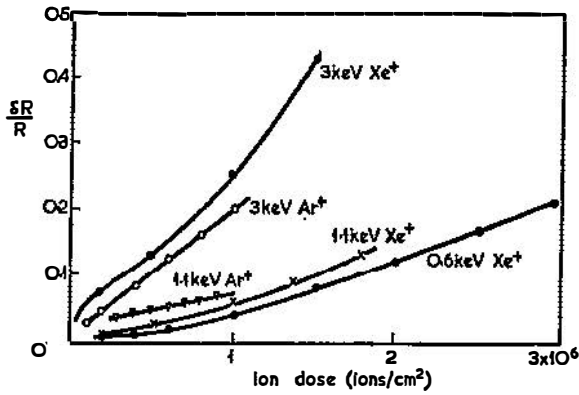


Fig. 2. Experimental sputtering curves.

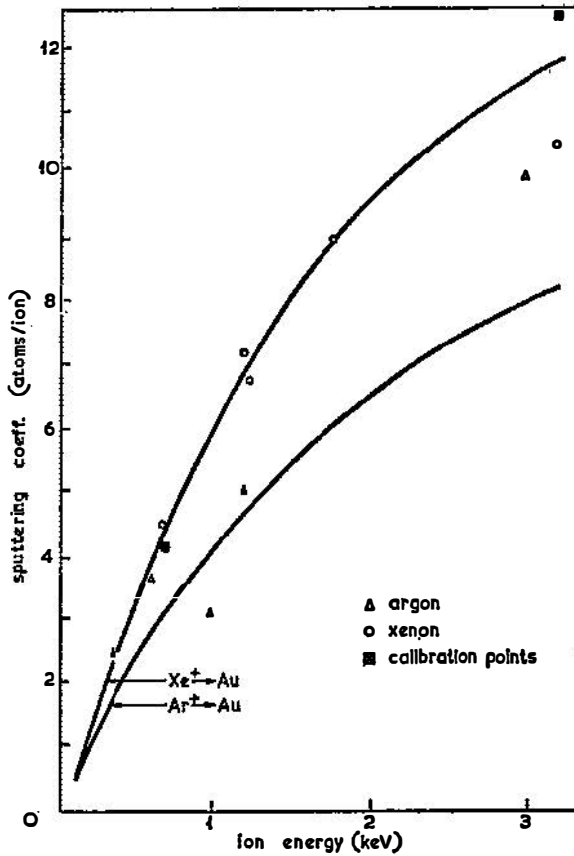


Fig. 3 Comparison of the present sputtering data with published data.

values of  $S$  by Wehner<sup>7)</sup> and with direct measures of  $S$  using the Talystep to determine the depth removed for given ion doses. Clearly agreement is good for both ion species, particularly so at lower ion energies and this gives confidence in using these sputtering coefficients at the lower ion dose level. It also indicates that resistance measurement techniques can be profitably used to measure sputtering coefficients of conductors.

c) Ion irradiation defect production.

We return now to consideration of the initial resistance increase and quasiequilibrium phases mentioned earlier. As noted previously, experiments in these regions were conducted using either one of the ion types at constant energy or one of the ion types at successively different energies. Initially the discussion will be concerned with irradiation at one fixed energy and it should be remembered that resistance was monitored while the ion beam was striking the target, so that resistance data were acquired in a dynamic state and did not, unless otherwise specified, depend upon a time interval after bombardment during which annealing could and did take place. The form of the resistance increase during bombardment is depicted in Fig. 4 for  $A^+$  bombarding  $\sim 600\text{\AA}$

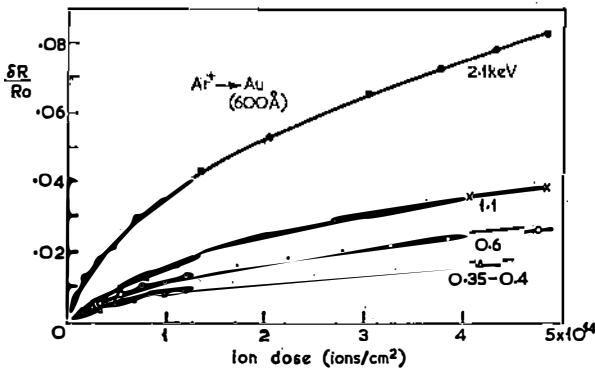


Fig. 4 The energy dependence of the composite  $\delta R/R_0/(\Phi)$  function.

gold films at energies up to 2.1 keV and the initial rapid rise and quasiequilibrium phases can be distinguished. In view of the earlier comments regarding sputter thinning of the films, raw data such as Fig. 4 were re-evaluated by adding to the measured resistance changes, values corresponding to the depth of film lost by sputtering. Since the data still indicated a quasi-saturation condition, it was initially assumed that the resistance change data could be adequately represented by a similar equation to that proposed by Merkle<sup>8)</sup> for resistance changes in MeV proton irradiated gold, i. e.

$$\frac{d(\delta\varrho)}{d\Phi} = L - M\delta\varrho, \quad (5)$$

where  $L$  and  $M$  are constants.

This expression may be rewritten

$$\frac{\delta R}{R_0} = A \{1 - \exp(-B\Phi)\}, \tag{6}$$

where  $A$  and  $B$  are further constants and  $A$  is the quasi-equilibrium fractional resistance change.

Consequently, data such as that of Fig. 4 were replotted in the form  $\log\left(1 - \frac{\delta R}{AR_0}\right)$  as a function of ion dose ( $A$  being taken from the quasi-equilibrium levels) with results such as shown in Fig. 5. Clearly equation (6) represents the behaviour of  $\delta R$  rather well over a large range of doses, except the

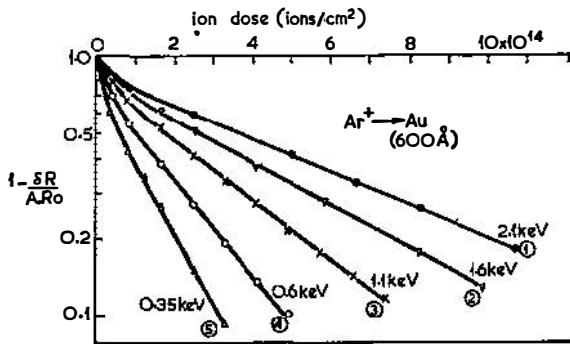


Fig. 5. The radiation damage curve, extracted from the composite functions of Fig. 4, fitted to a mathematical form.

initial portion, where the rate of resistance change is faster than predicted by equation (6). In the regime where equation (6) is obeyed the reciprocal of the dose constant  $B^{-1}$  was found to rise linearly with ion energy from  $1.5 \times 10^{15}$  ions/cm<sup>2</sup> at 300 eV to  $10 \times 10^{15}$  ions/cm<sup>2</sup> at 3 keV for  $A^+$  ions. Values of  $B^{-1}$  and the saturation dose level  $A$  were both lower for Xe ions. For all these measurements, it was found necessary to commence with virtually identical initial films, since increasing film thickness resulted in the expected reduction of resistance change rate, since the incident ions would penetrate and damage a smaller fraction of the film thickness. Additionally, experiments performed with films evaporated on to rock salt substrates rather than glass, in an attempt to obtain epitaxial films revealed only small differences in resistance change but further experiments are required to determine any real effects of film geometry.

In view of the fact that the experimental data cannot be fully represented by equation (6), a further technique of analysis was used in which  $\frac{\delta R}{R_0}$  was supposed to be composed of the summation of two exponential functions,

$A_1(1-\exp(-B_1\Phi))=x_1$  and  $A_2(1-\exp(-B_2\Phi))=y_1$ . Fig. 6 reveals the result of plotting two such functions,  $x_1$  and  $y_1$  for an arbitrary choice of  $A_1=A_2$  and  $B_1=10B_2$  and their summation in the form  $\left(1-\frac{x_1+y_1}{A_1+A_2}\right)$ . If this summed curve is compared with those of Fig. 5, it is immediately clear that, with a suitable choice of constants  $A_{1,2}$  and  $B_{1,2}$ , the double exponential form could be closely fitted to the experimental data, whereas a single exponential would

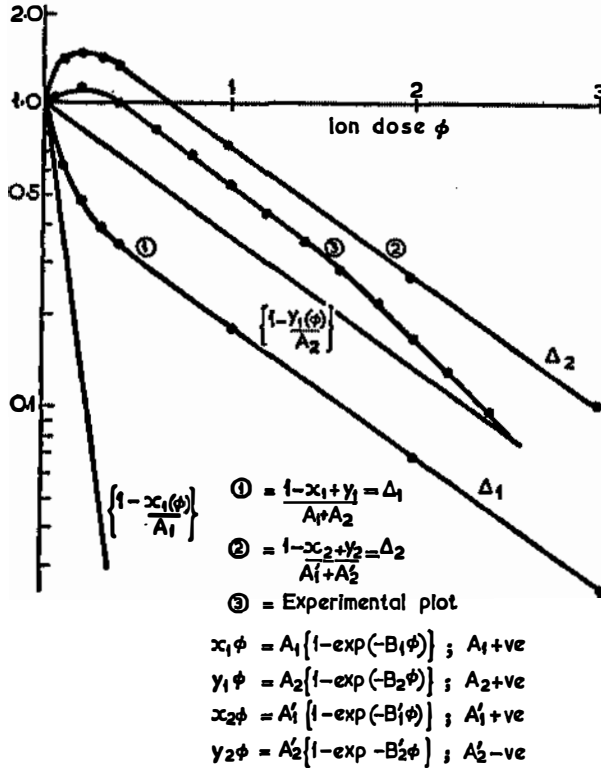


Fig. 6 The mathematical composition of:  
 1) 'Radiation damage' curve.  
 2) 'Radiation-annealing' curve.  
 3) Experimental plot of type 2.

fit in either the initial region or final region only. Although specific values of  $A_{1,2}$  and  $B_{1,2}$  have not been deduced, it is clear that  $B_2$  represents the value of  $B$  evaluated earlier and  $A_1+A_2$  represents the value of  $A$ . The most important conclusion to be drawn is that the resistance change function is composed of two build up functions which, as will be discussed later, suggests the production of two forms of defect centre which influence the resistance of the film.

During these constant energy bombardment experiments, it was observed in the same way as had Navinšek and Carter, that if bombardment was inter-

rupted and the film resistance monitored as a function of time, then the resistance of the film fell with increasing time to such a level that up to 10% of the resistance increase resulting from bombardment could be recovered and the characteristic time behaviour of the resistance recovery was of a simple exponential character. Upon restarting bombardment an initial rapid rise in resistance occurred, similar to that at the initiation of bombardment of the film but then the rate of rise declined until the resistance dose function coincided with an uninterrupted bombardment function. This suggests that there is a thermal recovery of some of the ion irradiation damage but that this damage can be rapidly restored by further bombardment.

As a result of this observation of damage restoration, a sequence of experiments was conducted in which films were initially bombarded with a more energetic ion (3 keV) and then the ion energy either suddenly reduced to a lower value or after the higher energy bombardment was ceased, lower energy bombardment commenced after a subsequent, measured, time interval. The effects of this process were quite remarkable and may be summarized as follows. When the second bombardment energy was much lower than the first (e.g. 300 eV after 3 keV) the resistance of the film was observed to decrease; when the second ion energy was not so much less than the first, the resistance increased but at a lower rate than would be the case if the higher energy bombardment had been continued and when the ion energies were equal, no change in rate was observed (except for restoration of the thermal loss in the case of a time delay between bombardments). These statements must be further amplified since, although a resistance decrease does occur with widely dissimilar bombardment energies, an initial increase or peak in resistance was also obtained before this decrease occurred.

The magnitude of this increase was reduced when the time delay between bombardments was decreased and, as shown in Fig. 7, is practically non-existent for a time delay of 7 s. This behaviour clearly suggests that the initial effect of the second bombardment is to restore some of the thermally annealed damage which recovers during the time delay. Furthermore, the resistance decrease was not indefinite, since as Fig. 7 shows, after long secondary bombardments the resistance passed through a minimum and subsequently increased but at a lower rate than with the first higher energy bombardment. It may be noted that the final slopes of all the curves in Fig. 7 are, in fact, very similar, indicating that any temporary effects have ceased and the systems have reached equilibrium under the second bombardment conditions. It was also observed that the greater the initial ion dose at the first energy, such that the resistance change was closer to quasi-equilibrium, the smaller the effects of a second bombardment at a lower energy, whilst increasing the first ion energy relative to the second causes the minima of Fig. 7 to increase towards higher second ion doses. At first, it was suspected that these phenomena were the result of surface contamination and ion beam decontamination processes but it was quickly established that this was not the case since, (1) no resistance decreases, a phenomenon previously associated with decontamination, were ever observed in the clean system and data shown unless the films had previously experienced a higher energy bombardment, (2) the magnitude of the resistance decrease diminished with increasing time delay between bombardments, in total contra-distinction to the effects anticipated if the surface became contaminated in this period and (3) measurements of changes in secondary emission coefficients during these

experiments were very much smaller than were experienced when deliberate film contamination was allowed. Consequently, we are led to postulate that the effects are the result of partial annealing of the damage induced by the first bombardment (which are responsible for resistance increases), by the second bombardment at lower energy. Simultaneous with this process, however, the second bombardment can create its own damage, as indicated by the restoration of thermally annealed damage and the initial increase or peak in resistance during second bombardment and the final increase in resistance following the resistance minima can be directly associated with sputtering of the film, as mentioned earlier.

Again, if it is assumed that the damage annealing process can be represented by an exponential function but with a negative coefficient  $A_1$ , then this can result in the negative resistance change during second ion bombardment as shown in Fig. 7 where both the annealing function with  $A_2$  negative and a da-

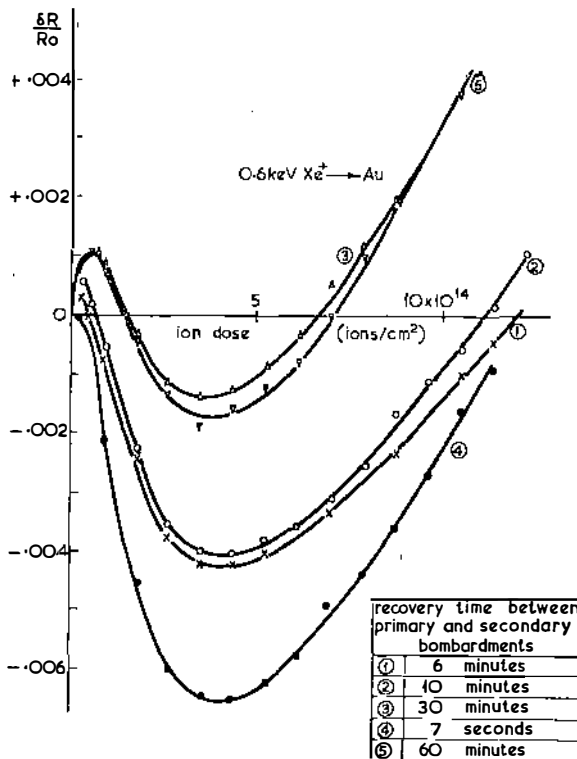


Fig. 7 The recovery time dependence of the initial peak occurring in radiation annealing experiments.

mage function with  $A_1$  positive and their summation, leads to the observed type of second ion bombardment curve as depicted by  $\Delta_2$ . Again, magnitudes have not yet been evaluated for the appropriate constants but the important fact is that clearly a radiation annealing process does take place as the earlier discussion similarly indicated the presence of two rates of damage production.

In order to offer explanations for these processes, we first accept, as has been proved in many electron irradiation experiments, that it is the introduction of defects to the lattice which results in a diminution of conduction electron mean free path with a consequent increase in electrical resistance. There is a clear difference between high energy electron irradiations, in which defects are produced homogeneously and at large spacing and low energy ion irradiations where the ion collision free paths are only of the order of atomic spacings, so that defects are produced in a dense cascade and at close separation. Under these circumstances, defect clustering of like defects and annihilation of unlike defects is expected and indeed, electron microscopic investigations<sup>4, 9-15)</sup> of gold films irradiated with low energy ions have confirmed the existence of clusters, in the form of dislocation loops, of both vacancy and interstitial character. In the vacancy case, it is probable that the loops are formed directly following the generation of a vacancy rich core in the displacement cascade but that for interstitial loops, it is necessary that the gold should contain impurities (such as the injected inert gas ion) which act as nucleation centres for randomly migrating interstitials also generated in the cascade. The main reason for resistance, increase in the ion bombardment case, therefore, appears to be due to defect cluster formation and the probable co-existence of two cluster types simultaneously can be considered to be an indication that two damage build up functions as suggested by the data of Fig. 5, may be anticipated.

In addition, for both types of defect cluster there will be defect annihilation processes occurring, such as sputtering of the dislocation loops where they intersect the surface, loss by slip and glide of these loops to the surface by image forces, accumulation of defects of opposite type by a cluster of defects and ejection of defects from clusters by incident ions or knock ons. Although magnitudes of these effects are difficult to estimate, there is clear evidence for their simultaneous operation (e.g. electron microscopic observations of Thomas et al<sup>15)</sup> of cluster loss close to the surface of thin gold films by the image force processes).

The important point is that each and all of these processes leads to a net decrease in damage and the appropriate conditions for damage saturation, at sufficiently large ion doses are established, as can be inferred to occur in the present work from the exponential build up of resistance functions to quasi equilibrium level.

Damage loss processes may be expected to become of decreasing importance as the depth of damage from the free surface increases since, for example, image forces decline rapidly and the energy of ions and recoils, available for cluster depletion, will diminish deeper in the solid. Thus, the damage rates and saturation levels would be expected to increase with increasing ion energy and decreasing ion mass, since the ion range and therefore the depth of damage production increases with these changes in the energy and mass parameters. As shown earlier, this is precisely the behaviour observed in the resistance change functions.

Since the resistance change curves are composed of two dose functions, it is reasonable to suppose that each of these functions represents the build up of one type of defect cluster. Electron microscopic observations<sup>14)</sup> of cluster production indicate that only at *low* ion doses can vacancy clusters be unequivocally identified whilst interstitial clusters are generally observed at higher ion doses ( $\sim 10^{15}$  ions/cm<sup>2</sup>). The reasons for such behaviour need not concern us

here but arise both from the fact that vacancies and interstitials migrate at different rates, and have different cross sections for capture of a like defect to nucleate clustering and that substantial impurity content is required in the sample to nucleate interstitial growth. These observations suggest that in the present work, the initial rapid resistance change, at low ion doses, is the result of vacancy cluster formation, whilst at higher ion doses, the vacancy cluster density saturates and interstitial cluster growth is more important until their saturation occurs also. The thermal annealing behaviour discussed earlier indicates that either or both types of cluster has a certain instability at room temperature and in view of the fact that damage restoration apparently occurs at the initial rapid rate after thermal annealing by further constant energy bombardment, it is suggested that it is the vacancy cluster which undergoes thermal anneal and subsequent reformation.

In order to understand the radiation anneal behaviour, it should be noted that an ion of high energy will produce damage into the film as far as its own depth of penetration and further still by recoil atoms and on diffusing defects.

At saturation, the damage production and annihilation processes will be in equilibrium to the depth of defect production and migration. When the ion energy is lowered and no thermal anneal has occurred, then ions will only be able to maintain an equilibrium between production and annihilation to a shallower depth but shot on and migrating defects will be able to travel into the film beyond this depth into the damage created by the earlier, more energetic ions. As far as the second lower energy ions are concerned, this deeper region will be super-saturated with damage and the shot on defect will be to anneal this region. Consequently, an anneal will occur of the deeper lying damage, whilst a new equilibrium will be established nearer the surface. The net effect will be an initial reduction in resistance, as observed. If thermal anneal has occurred, however, then the second ion will re-establish its own equilibrium concentration of this type of cluster (probably vacancy) near the surface, at the same time as annealing deeper lying damage. Hence the reason for the initial rise in resistance if thermal annealing occurred between bombardments.

Since both vacancies and interstitials are produced by the bombardment, then both species will be available for damage anneal beyond the lower energy ion range. The interstitial migration rate in gold is many orders of magnitude faster at room temperature than the vacancy rate, thus there is a stronger chance of interstitial escape from the damage zone than vacancy escape. As a consequence, it is believed that the vacancies produced beyond the lower energy ion range migrate to interstitial clusters and cause their partial annihilation. For large differences in energy between the first and second bombarding ions the supersaturation levels beyond the second ion range would be large but as the two energies become more nearly equal, the relative supersaturation would decrease. This would lead, as observed, to larger radiation annealing for widely different energies than for smaller energy differences and would also indicate that more annealing would occur (and thus the resistance change minima move to higher second ion doses) with increasing primary ion energy, again as observed. Finally, when the primary ion dose itself has been insufficient to cause saturation, the radiation anneal should be lower, since less clusters are available for annihilation, this again corresponds to the measured resistance change behaviour.

Consequently, although the magnitudes of the effects described here have not been evaluated, the present suggestions indicate that not only can energetic ions produce both vacancy and interstitial clusters, the former being capable of at least partial thermal anneal at room temperature but that a radiation anneal mechanism must also operate. In this work, it is believed that the anneal of damage created by initial more energetic ions by a second lower energy ion is a result of interstitial cluster annihilation by vacancies generated by the lower energy ion.

Quite clearly, some of these suggestions are speculative and a more direct confirmation would be attained by direct electron microscopic observations of defect production and by further studies at different temperatures and solids with different defect migration properties. Such parallel experiments are now engaging our attention.

#### A c k n o w l e d g m e n t

A. R. Bayly would like to thank the Science Research Council for provision of a maintenance grant during the course of these studies.

#### R e f e r e n c e s

- 1) For a review of electron bombardment studies see for example „The Ion Bombardment of Solids“ by G. Carter and J. S. Colligon, Heinemanns, London, 1968.
- 2) V. Teodosić, *Appl. Phys. Letters*, **9** (1966) 209;
- 3) B. Navinšek and G. Carter, *Can. J. Phys.*, **46** (1968) 719;
- 4) B. Jouffrey, Ph. D. Thesis, University of Paris (1964);
- 5) For a review of this work, see ref. 1).
- 6) K. L. Chopra and M. R. Randlett, *J. Appl. Phys.*, **38** (1967) 3144;
- 7) G. K. Wehner, General Mills Electronics Group, Report No 2309, (1962);
- 8) X. L. Merkle, *Proc. Int. Conf. on Solid State Physics Research with Accelerators*, Brookhaven, U.S.A. (1967);
- 9) G. J. Ogilvie, J. V. Sanders and A. A. Thomson, *J. Phys. Chem. Solids*, **24** (1963) 247;
- 10) J. A. Venables and R. W. Balluffi, *Phil. Mag.*, **11** (1965) 1021 and 1039;
- 11) P. B. Bowden and D. G. Brandon, *Phil. Mag.*, **8** (1963) 935;
- 12) J. Diehl, H. Diepers and B. Hertel, *Can. J. Phys.*, **46** (1968) 647;
- 13) L. E. Thomas and R. W. Balluffi, *Phil. Mag.*, **15** (1967) 1117 and 1137;
- 14) G. Högberg, and H. Norden, (1970) to be published;
- 15) L. E. Thomas, T. Schober and R. W. Balluffi, *Radiation Effects*, **1** p. 257, 269 and 279.

## 2.8 Influence of the type of bombarding ions on the change of resistivity of bombarded thin metal layer

V. M. TEODOSIĆ, *Electrical Engineering Faculty, University of Beograd, Beograd, Yugoslavia*